



XXVIIth International Conference on Ultrarelativistic Nucleus-Nucleus Collisions
(Quark Matter 2018)

Higher moment fluctuations of identified particle distributions from ALICE

Nirbhay Kumar Behera for the ALICE collaboration

Inha University, 100, Inharo, Namgu, Incheon, South Korea

Abstract

Cumulants of conserved charges fluctuations are regarded as a potential tool to study the criticality in the QCD phase diagram and to determine the freeze-out parameters in a model-independent way. At LHC energies, the measurements of the ratio of the net-baryon (net-proton) cumulants can be used to test the lattice QCD predictions. In this work, we present the first measurements of cumulants of the net-proton number distributions up to 4th order in Pb–Pb collisions at $\sqrt{s_{NN}} = 2.76$ and 5.02 TeV as a function of collision centrality. We compare our cumulant ratios results with the STAR experiment net-proton results measured in the first phase of the Beam Energy Scan program at RHIC. The results can be used to obtain the chemical freeze-out parameters at LHC.

Keywords: Fluctuations, conserved quantum number, freeze-out parameters, lattice QCD, ALICE, LHC.

1. Introduction

The study of fluctuations of conserved charges in heavy-ion collision experiments is regarded as an excellent observable to map the QCD phase diagram. Heavy-ion collision experiments at LHC energies aim to explore the QCD phase diagram at the chiral limit, where the baryo-chemical potential (μ_B) is very small. According to lattice QCD, the phase transition is a crossover at vanishing μ_B [1]. It has been also proposed that at the chiral limit of light quarks, the phase transition is of the second order, belonging to the universality class of 3-dimensional O(4) spin model [2]. Based on this model, the chiral crossover transition line will appear close to the freeze-out line. Therefore, the determination of freeze-out parameters is very important to locate the phase boundary at LHC energies. The freeze-out parameters are obtained by fitting the particle yields and then comparing them with thermal statistical models like the Hadron Resonance Gas (HRG) model [3]. Recently, the chemical freeze-out temperature is estimated as 156.5 ± 1.5 MeV at LHC energy by a statistical hadronization model using the ALICE particle yields [4]. On the other hand, the crossover temperature, T_c , estimated by lattice QCD calculations is 155 (1) (8) MeV [5]. It can be observed from the thermal model and from lattice QCD calculations that the freeze-out temperature is close to the crossover temperature. Hence, additional measurements of the freeze-out temperature are needed to test the lattice QCD predictions

Experimentally measured cumulants (C_n) of conserved charge distributions, like net-charge and net-baryons can be directly connected with various quark number susceptibilities ($\chi_q^{(n)}$) as $C_n = VT^3\chi_q^{(n)}$ [6]. Here the quark number susceptibilities are given by -

$$\chi_q^{(n)} = \frac{\partial^n [P(T, \mu)/T^4]}{\partial(\mu_q/T)^n} . \quad (1)$$

In Eq. 1, P is the pressure, T is the temperature and V is the volume of the system. To get rid of the volume term in Eq. 1, the freeze-out parameters can be determined by taking the ratio of the various orders of cumulants [2, 6].

In this work the cumulants of net-proton number fluctuations up to 4th order in minimum-bias Pb–Pb collisions at $\sqrt{s_{NN}} = 2.76$ and 5.02 TeV are reported. The ratio of cumulants, C_3/C_2 and C_4/C_2 are compared with Skellam expectations as a function of centrality. They are also compared with RHIC Beam Energy Scan (BES) results.

2. Experimental setup and analysis methodology

The analysis is carried out using data from Pb–Pb collisions recorded at $\sqrt{s_{NN}} = 2.76$ and 5.02 TeV with the ALICE detector [7]. Around 14×10^6 and 59×10^6 minimum-bias events are used for this analysis at $\sqrt{s_{NN}} = 2.76$ and 5.02 TeV, respectively. The V0 detectors covering the pseudorapidity ranges $2.8 < \eta < 5.1$ (V0A) and $-3.7 < \eta < -1.7$ (V0C) are used for the trigger and centrality estimation. A minimum-bias trigger is defined by the coincidence of a signal in both the V0A and V0C. The events are classified into different centrality classes using the V0 signal amplitudes [8]. To reject the background events and secondary interactions, only events with a reconstructed primary vertex (V_z) < 10 cm from the center of the ALICE coordinate system (along the z-direction) are considered. The contribution from pileup events for Pb–Pb collisions $\sqrt{s_{NN}} = 2.76$ TeV is negligible, while for 5.02 TeV data the pileup events are removed using the correlation between number of hits in Silicon Pixel Detector (SPD) and the multiplicity of V0 detector. For this analysis, tracks reconstructed using the Time Projection Chamber (TPC) with transverse momentum (p_T) range $0.4 < p_T < 1.0$ GeV/c and pseudorapidity range of $-0.8 < \eta < 0.8$ are selected. To ensure good quality tracks, the following criteria are applied. The reconstructed tracks are selected with at least 80 out of 159 space points in the TPC. Reconstructed tracks have been selected requiring a good quality fit ($\chi^2/NDF < 4$). Tracks associated to weak leptonic decay topologies are rejected. Furthermore, a p_T dependent selection criteria based on the distance of closest approach (DCA) is imposed to minimize the contribution from secondaries and weak decays. For the (anti-)proton identification the specific ionization energy-loss (dE/dx) information of a given track in TPC volume is used. A condition of $|n\sigma| < 2.5$ around the expected mean values of dE/dx for (anti-)proton is applied. The contamination due to particle misidentification for $p_T < 0.85$ GeV/c is negligible, and for $0.85 < p_T < 1.0$ GeV/c is around 10%. This effect is taken into account in the systematic uncertainties.

The p_T dependent proton (p) and anti-proton (\bar{p}) reconstruction efficiencies are estimated by means of a full Monte Carlo simulation, using the HIJING event generator and the GEANT3 transport code, followed by the standard reconstruction procedure [9, 10]. The reconstruction efficiency of p and \bar{p} are about 65% and 60%, respectively. The efficiency correction of the $\langle p \rangle$, $\langle \bar{p} \rangle$ numbers and the cumulants of net-proton distributions are done using the method proposed in Ref. [11]. The statistical uncertainties are estimated using the Subsample method with 30 subsamples. The systematic uncertainties are estimated by varying the track quality and V_z selection criteria with respect to the default ones. The final results reported here are corrected for the centrality bin width [12].

3. Results and discussion

The second, third and fourth order cumulants of net-proton distributions in Pb–Pb collisions at $\sqrt{s_{NN}} = 2.76$ and 5.02 TeV are shown in Figure 1 as a function of centrality. It can be observed from Figure 1 that the C_2 and C_4 of net-proton distributions are decreasing from central to peripheral events, while C_3 does

not show a strong centrality dependence. These results are the same, within the uncertainties, for both the energies.

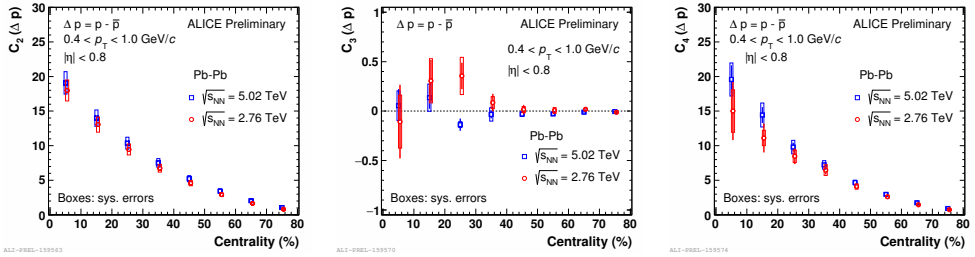


Fig. 1. (From left to right) Centrality dependence of C_2 , C_3 and C_4 of net-proton distributions in Pb–Pb collisions at $\sqrt{s_{NN}} = 2.76$ and 5.02 TeV. The vertical lines and boxes represents the statistical and systematic uncertainties, respectively.

In Figure 2, C_3/C_2 and C_4/C_2 of net-proton distributions in Pb–Pb collisions at $\sqrt{s_{NN}} = 2.76$ and 5.02 TeV are shown as a function of collision centrality. The results are compared with Skellam expectations. If the numbers of protons and anti-protons are distributed according to two independent Poissonians, then the net-proton number will follow a Skellam distribution. The cumulants C_n of a Skellam distributions are given as, $C_n = C_1(p) + (-1)^n C_1(\bar{p})$. The dotted lines in Figure 2 represent the Skellam expectations. It can be seen from Figure 2 that values of C_3/C_2 are within the Skellam expectations for energies in all centrality bins considering the uncertainties. In central and semi-central events, values of C_4/C_2 of net-proton number fluctuations agree with Skellam expectations. However, some significant deviations from the Skellam line is observed in peripheral events, which will be the subject of future investigations.

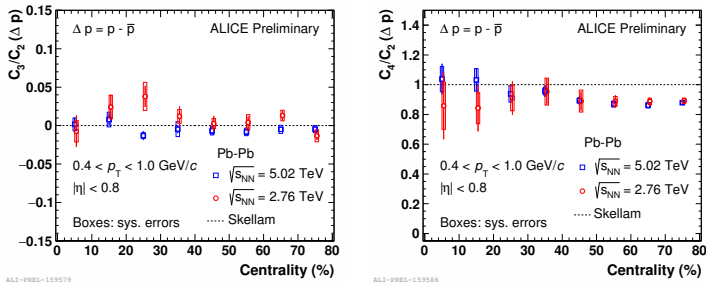


Fig. 2. Centrality dependence of C_3/C_2 and C_4/C_2 of net-proton distributions in Pb–Pb collisions at $\sqrt{s_{NN}} = 2.76$ and 5.02 TeV. The vertical lines and boxes represents the statistical and systematic uncertainties, respectively.

We also compare our results with RHIC BES results of net-proton measured in $0.4 < p_T < 0.8$ GeV/c and $|\eta| < 0.5$ [13]. The beam energy dependent results of C_3/C_2 and C_4/C_2 are shown for the most central collisions in Figure 3. It should be noted that our results are obtained in $0.4 < p_T < 1.0$ GeV/c and pseudorapidity range $-0.8 < \eta < 0.8$. However, using the RHIC kinematic ranges has a minimal influence on our results. It can be seen that going from RHIC to LHC energy, values of C_3/C_2 and C_4/C_2 of net-proton number fluctuations approach Skellam expectations within the relatively small kinematic window.

4. Summary

In these proceedings, we presented the first measurements of net-proton cumulants up to 4th order and their ratios in Pb–Pb collisions at $\sqrt{s_{NN}} = 2.76$ and 5.02 TeV as a function of centrality. Within the cur-

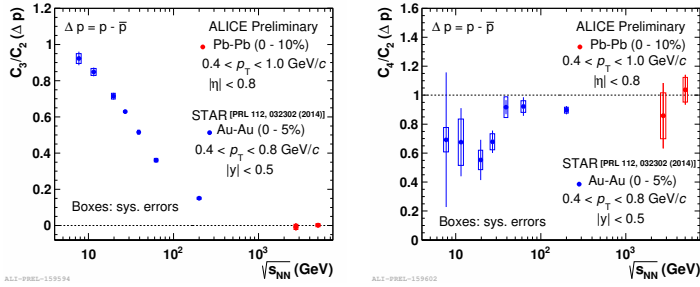


Fig. 3. Energy dependence of C_3/C_2 and C_4/C_2 of net-proton distributions for the most central collisions.

rent kinematic cuts, the cumulant ratios (C_3/C_2 , C_4/C_2) results are found to be consistent with Skellam expectations within the uncertainties. We also compared our results concerning the net-proton cumulants with those obtained at RHIC by the STAR experiment with the BES program. From RHIC to LHC, the ratio approaches the Skellam expectations. The upcoming dedicated Pb–Pb run at 5.02 TeV will improve the statistical precision to further constrain the freeze-out parameters. The study of higher order cumulants of net-charge and net-kaon in a wide kinematic region is also a subject of future investigations.

5. Acknowledgements

This work was supported by National Research Foundation of Korea (NRF), Basic Science Research Program through the National Research Foundation of Korea funded by the Ministry of Education, Science and Technology (Grant number: NRF-2014R1A1A1008246).

References

- [1] Y. Aoki, G. Endrodi, Z. Fodor, S. D. Katz and K. K. Szabo, *Nature* **443**, 675 (2006).
- [2] B. Friman, F. Karsch, K. Redlich and V. Skokov, *Eur. Phys. J. C* **71**, 1694 (2011).
- [3] A. Andronic, P. Braun-Munzinger and J. Stachel, *Acta Phys. Polon. B* **40**, 1005 (2009).
- [4] A. Andronic, P. Braun-Munzinger, K. Redlich and J. Stachel, *J. Phys. Conf. Ser.* **779**, no. 1, 012012 (2017)
- [5] T. Bhattacharya *et al.*, *Phys. Rev. Lett.* **113**, no. 8, 082001 (2014).
- [6] F. Karsch and K. Redlich, *Phys. Lett. B* **695**, 136 (2011).
- [7] K. Aamodt *et al.* [ALICE Collaboration], *JINST* **3**, S08002 (2008).
- [8] K. Aamodt *et al.* [ALICE Collaboration], *Phys. Rev. Lett.* **106**, 032301 (2011).
- [9] X. N. Wang and M. Gyulassy, *Phys. Rev. D* **44**, 3501 (1991).
- [10] R. Brun, F. Carminati, and S. Giani, CERN-W5013 (1994).
- [11] T. Nonaka, M. Kitazawa and S. Esumi, *Phys. Rev. C* **95**, no. 6, 064912 (2017).
- [12] X. Luo, J. Xu, B. Mohanty and N. Xu, *J. Phys. G* **40**, 105104 (2013).
- [13] L. Adamczyk *et al.* [STAR Collaboration], *Phys. Rev. Lett.* **112**, 032302 (2014).